

R.J. Stouffer · S. Manabe

# Equilibrium response of thermohaline circulation to large changes in atmospheric CO<sub>2</sub> concentration

Received: 21 May 2002 / Accepted: 6 November 2002 / Published online: 4 March 2003  
© Springer-Verlag 2003

**Abstract** This study evaluates the equilibrium response of a coupled ocean–atmosphere model to the doubling, quadrupling, and halving of CO<sub>2</sub> concentration in the atmosphere. Special emphasis in the study is placed upon the response of the thermohaline circulation in the Atlantic Ocean to the changes in CO<sub>2</sub> concentration of the atmosphere. The simulated intensity of the thermohaline circulation (THC) is similar among three quasi-equilibrium states with the standard, double the standard, and quadruple the standard amounts of CO<sub>2</sub> concentration in the atmosphere. When the model atmosphere has half the standard concentration of CO<sub>2</sub>, however, the THC is very weak and shallow in the Atlantic Ocean. Below a depth of 3 km, the model oceans maintain very thick layer of cold bottom water with temperature close to  $-2^{\circ}\text{C}$ , preventing the deeper penetration of the THC in the Atlantic Ocean. In the Circumpolar Ocean of the Southern Hemisphere, sea ice extends beyond the Antarctic Polar front, almost entirely covering the regions of deepwater ventilation. In addition to the active mode of the THC, there exists another stable mode of the THC for the standard, possibly double the standard (not yet confirmed), and quadruple the standard concentration of atmospheric carbon dioxide. This second mode is characterized by the weak, reverse overturning circulation over the entire Atlantic basin, and has no ventilation of the entire subsurface water in the North Atlantic Ocean. At one half the standard CO<sub>2</sub> concentration, however, the intensity of the first mode is so weak that it is not certain whether there are two distinct stable modes or not. The

paleoceanographic implications of the results obtained here are discussed as they relate to the signatures of the Cenozoic changes in the oceans.

## 1 Introduction

General circulation models of the coupled ocean–atmosphere system have been extensively used to predict the future climate changes. Analyzing the transient response of a coupled ocean–atmosphere model to a gradual increase in the atmospheric concentration of carbon dioxide over a period of 100 years, Stouffer et al. (1989) and Manabe et al. (1991) noted that, in the Atlantic Ocean, the simulated thermohaline circulation (THC) slowly weakens with time. Although there are few exceptions, the weakening of the THC also occurred in the time integration of many coupled models as described in the reports of the Intergovernmental Panel on Climate Change (1991, 1995, 2001).

Following the study mentioned, Manabe and Stouffer (1993, 1994) extended the time integration of the model beyond 100 years, and investigated the multi-century response of the THC to the doubling and quadrupling of the atmospheric carbon dioxide. In these experiments, the CO<sub>2</sub> concentration initially increased at the rate of 1% per year, but stopped increasing when it is doubled or quadrupled and did not change thereafter over a period of several hundred years.

In the CO<sub>2</sub>-doubling experiment mentioned, the THC in the Atlantic Ocean weakened initially but began to re-intensify several decades after the CO<sub>2</sub> concentration was stabilized at twice its standard value. A few hundred years later, it regained its initial intensity. When the CO<sub>2</sub>-doubling experiment was time-integrated to a near equilibrium state (Stouffer and Manabe 1999), the THC maintained its original intensity. In the quadrupling experiment, the THC initially weakened in a manner similar to the CO<sub>2</sub>-doubling experiment. A few hundred

---

R.J. Stouffer (✉)  
Geophysical Fluid Dynamics Laboratory/NOAA,  
PO Box 308, Forrestal Campus, Princeton University,  
Princeton, NJ 08542, USA  
E-mail: Ronald.Stouffer@noaa.gov

S. Manabe  
Program in Atmospheric and Oceanic Sciences,  
Princeton University, PO Box CN710, Sayre Hall, Forrestal  
Campus, Princeton, NJ 08544-0710, USA

years later, however, its intensity became very weak and remained so until the end of the experiment (i. e., the 500th year).

Using an ocean general circulation model coupled to an energy moisture balance model of the atmosphere, Wiebe and Weaver (1999) performed a set of experiments, which were similar to the CO<sub>2</sub>-doubling and CO<sub>2</sub>-quadrupling experiments mentioned. In both experiments, the THC initially weakened, but then started to intensify, eventually acquiring an intensity, which is significantly stronger than the original intensity.

These results presented imply that the initial response of the THC does not necessarily indicate what follows thereafter. In the present study, the time integration of the coupled model continued over several thousand years so that the coupled model has enough time to approach its state of equilibrium. The main goal of the present study is to simulate the final equilibrated response of the THC to large changes in the atmospheric carbon dioxide and investigate the physical mechanisms involved.

Earlier, Manabe and Bryan (1985) investigated the equilibrium responses of a coupled model to large changes in atmospheric CO<sub>2</sub> concentration. The coupled model they used, however, has an idealized geography and the sector computational domain bounded by the equator and two meridians (120° longitude apart) between which the cyclic continuity is imposed. In view of the idealization of the model identified, it is desirable to reevaluate some of the results they obtained. The present study represents a renewed attempt to revisit this research topic using a coupled ocean-atmosphere model with realistic geography and global computational domain.

The equilibrium response study of the coupled ocean-atmosphere model conducted here could be used for understanding past as well as future changes of the oceans. In Sect. 7, the paleoceanographic implications of the results obtained here are discussed using various signatures of Cenozoic changes of the oceans.

---

## 2 Model structure

Manabe et al. (1991) described the basic structure of the model used here. It consists of general circulation models (GCM) of the atmosphere and oceans, and a simple model of continental surface. It is a global model with realistic geography limited by its computational resolution. It has nine unevenly spaced, vertical finite-difference levels. The horizontal distributions of predicted variables are represented by spherical harmonics of 15 associated Legendre functions for each of 15 Fourier components (rhomboidal 15 truncation) and by grid-point values (Gordon and Stern 1982). The vertical transfer of sensible and latent heat through moist convection is represented by a simple scheme called "moist convective adjustment" (Manabe et al. 1965). Insolation varies seasonally, but not diurnally. The model predicts cloud cover, depending only on relative humidity. A bucket model is used to compute the budgets of water and heat at continental surface (Manabe 1969).

The oceanic GCM (Bryan and Lewis 1979) uses a finite-difference technique and has a regular grid system with approximately a 4° latitude by 3.7° longitude spacing. There are 12 vertical

finite-difference levels. This oceanic component of the model interacts with the atmospheric counterpart once each day through exchanges of heat, water, and momentum. A simple sea-ice model (Bryan 1969) is also incorporated into the coupled model. It predicts sea-ice thickness using a thermodynamical model of sea ice, which moves with surface ocean currents unless sea-ice is thicker than 4 m and surface currents are converging. In addition, it is assumed that sea ice does not grow thicker than 10 m. This assumption prevents indefinite growth and eventual grounding of sea ice, which the present model cannot handle properly.

For details about the coupled ocean-atmosphere-land surface model, which is going to be called the "coupled model" for simplicity here, see Manabe et al. (1991).

As described, the model used here has low computational resolution and simple parameterization of various physical processes. Therefore, it is possible to time-integrate the model over many thousand of model years on current generation computers. To date, we are not aware of any other coupled general circulation model that has been integrated for more than 3000 years. Here, we present results from six separate time integrations, each more than 4000 years in length, some more than 10,000 years (Hall and Stouffer 2001).

---

## 3 Numerical time integrations

The initial condition for the time integration of the coupled model was obtained from separate time integrations of the atmospheric and oceanic components of the model. For the integration of the atmospheric component, the observed distribution of seasonally varying sea surface temperature is used as a lower boundary condition. For the oceanic integration, we used as the upper boundary conditions the observed distributions of sea surface temperature and salinity, and the computed distribution of surface wind stress, which are obtained from the atmospheric component of the model mentioned. Here, the seasonal cycle is represented via interpolation in time between monthly mean fields. Both integrations are conducted over a sufficiently long time for the component models to closely approach an equilibrium state. Combining the quasi-equilibrium states of the atmospheric and oceanic components of the model thus obtained, the initial condition for the time integration of the coupled model is constructed.

When the time integration of a coupled model starts from the initial conditions identified, the model climate tends to drift toward its own less realistic equilibrium state, yielding unrealistic distributions of sea ice as well as sea surface temperature and salinity. Such a drift can lead to a less realistic control climate, distorting the sensitivity of the model climate. To reduce the drift, the fluxes of heat and water at the ocean-atmosphere interface are adjusted at each grid point by given amounts before they are imposed upon the oceanic surface (see Manabe et al. 1991 for details). These adjustments do not change from one year to the next, and are independent of the fluctuating anomalies of surface temperature and salinity, which develop during the time integration of the coupled model. Thus, they neither systematically damp nor amplify these surface anomalies. Although the adjustments do not eliminate the shortcomings of model dynamics or thermodynamics

(Marotzke and Stone 1995), they reduce markedly the drift of the model from realistic initial conditions.

The flux adjustment technique may distort the results substantially when it is applied to a state, which is markedly different from the control state. For example, the state reached toward the end of the experiment with one half the standard CO<sub>2</sub> concentration is much colder than the control and has a very extensive coverage of thick sea ice in the Circumpolar Ocean of the Southern Hemisphere. If the sign of heat flux adjustment is negative (removing heat from the ocean) in regions with thick sea ice, indefinite sea-ice growth can occur. Imposing an upper limit of 10 m on the sea-ice thickness prevents the unconstrained growth in our model. However, the results obtained using such a constraint should be regarded with caution.

As described, the initial conditions for the control integration, which was extended more than 15,000 years, have realistic seasonal and geographical distributions of surface temperature, surface salinity, and sea-ice thickness, with which both the atmospheric and oceanic components of the model are nearly in equilibrium. The initial conditions, which are used for other integrations, are the states of the coupled model near the beginning of the control integration. Identical flux adjustments are applied to all integrations.

Throughout the course of the control integration, the atmospheric concentration of CO<sub>2</sub> was fixed at a value of 300 ppm by volume. In the three other integrations, CO<sub>2</sub> concentration increased or decreased initially from this value at the rate of 1%/year but remained unchanged after it reached twice, four times or one half the standard value of 300 ppm, respectively (Fig. 1). For ease of identification, these four integrations are going to be identified as control (1×C), 2×C, 4×C and 1/2×C, respectively. The time integration was performed over the period of more than 15,000 years for the control,

about 4000 years for the 2×C, and about 5000 years for the 4×C and 1/2×C cases, respectively.

Towards the end of all four integrations, the global mean temperature of the deepwater at the depth of 3 km ceased to change with time (Fig. 2), indicating that the model-ocean is close to the state of equilibrium. In the 1/2×C case, the temperature of deepwater stabilized at -1.9 °C earlier than other experiments as cold water sank and occupied the deeper layer of oceans. For the detailed analysis conducted here, we chose the mean states of the coupled model, which are obtained averaging over the last 100-year segment of the four integrations.

In addition to the four numerical experiments identified, we conducted two additional experiments. For the description of these two experiments, see Sect. 6.

#### 4 Thermal structure

In order to explore the equilibrium response of surface air temperature to large changes in atmospheric CO<sub>2</sub> concentration, Figure 3 is constructed. It illustrates the latitudinal profiles of zonal mean surface air temperature, which are obtained from the control (1×C), 2×C, 4×C, and 1/2×C experiments as described in the preceding section.

When interpreting the results of the numerical experiments conducted here, it is desirable to keep in mind that radiative forcing of climate due to the CO<sub>2</sub>-doubling hardly depends upon the CO<sub>2</sub> concentration in the atmosphere. For example, the doubling of CO<sub>2</sub> concentration from 150 to 300 ppm by volume has practically the same effect on the radiative forcing as the doubling from 300 to 600 ppm, or from 600 to 1200 ppm by volume.

Figure 3 shows that, in each doubling of CO<sub>2</sub> concentration from the 1/2×C to 1×C, from 1×C to 2×C, or

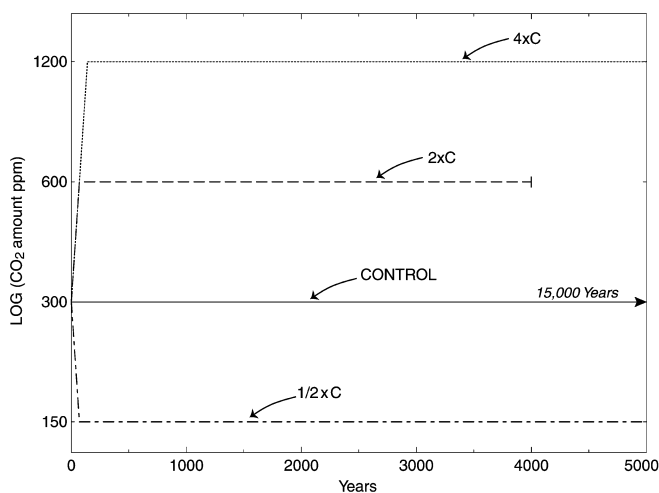


**Fig. 1** Temporal variation of CO<sub>2</sub> concentration of the atmosphere prescribed for the control (solid line), 2×C (dashed line), 4×C (dotted line), and 1/2×C (dash-dotted line)

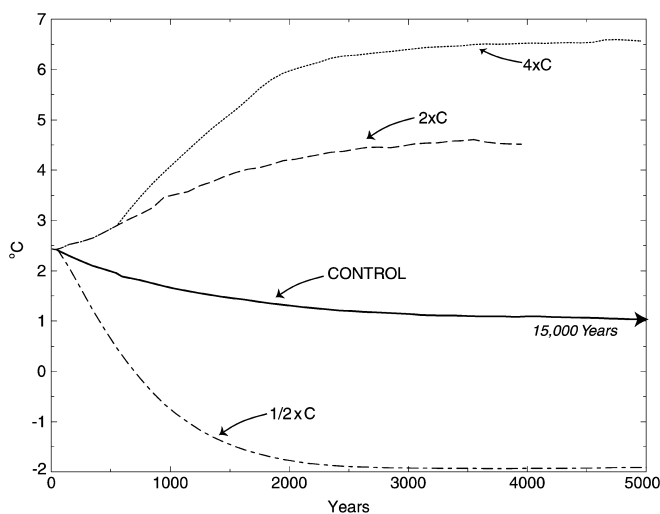


**Fig. 2** Temporal variation of globally averaged deep-water temperature at the depth of 3 km. Solid line: control; dashed line: 2×C; dotted line: 4×C; dash-dotted line: 1/2×C

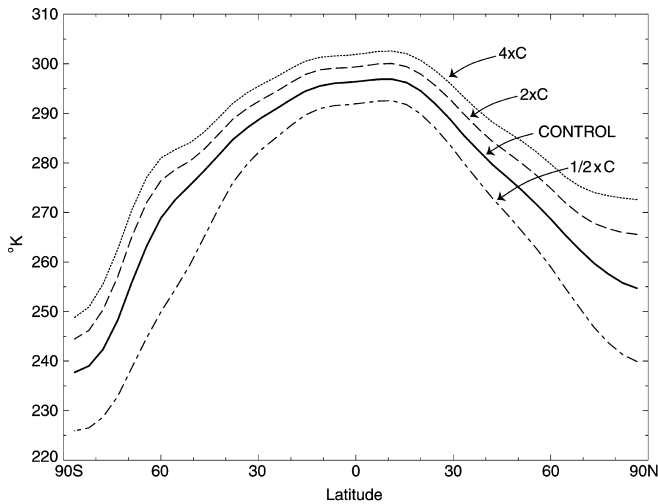


**Fig. 3** Latitudinal profiles of time mean surface air temperature (K), zonally averaged over both oceans and continents. The time mean is taken over the last 100 years of each experiment. *Solid line*: control; *dashed line*: 2×C; *dotted line*: 4×C; *dash-dotted line*: 1/2×C

**Table 1** Global mean surface air temperature (K) averaged over the last 100 years period of each experiment, and its the difference (°C) (individual minus the control (1×C) experiments)

	1/2×C	1×C	2×C	4×C
Global mean temperature	276.37	284.22	288.65	292.12
Difference	-7.85	0	+4.33	+7.90

from 2×C to 4×C experiments, the response of surface temperature increases with increasing latitudes. In high latitudes, where surface temperature is low, the albedo feedback process involving snow and sea ice enhances the change in surface temperature at high latitudes.

This figure also indicates that, in general, the equilibrium response of surface temperature to the change in CO<sub>2</sub> concentration by a given factor increases with decreasing surface temperature. For example, the difference in equilibrium surface air temperature between the 1/2×C and control cases is much larger than the difference between the control and the 2×C cases, which, in turn, is larger than the difference between the 2×C to the 4×C cases. Averaged over the entire globe, the difference in global mean surface temperature between the control and the 1/2×C case is almost as large as the difference between the control and 4×C case (Table 1). In short, a cold climate is much more sensitive than warm climate because of the large positive albedo feedback effect involving extensive snow and sea ice (Spelman and Manabe 1984).

The distributions of zonal mean oceanic temperatures, which are obtained from the set of experiments conducted here, are illustrated in latitude-depth frame (Fig. 4). As the CO<sub>2</sub> concentration is reduced from the 4×C to the 1/2×C levels, deepwater temperatures decrease. In the 1/2×C case, the very thick, cold layer of

bottom water with temperatures close to -2 °C extends all the way to high northern latitudes. The temperature of bottom water in the 1/2×C experiments is very close to what Schrag et al. (1996) estimated for the last glacial maximum based upon the isotopic analysis of pore water from tropical Atlantic sediments.

It is notable that, during the latter half of the 1/2×C experiment, very extensive, thick sea ice develops in the Circumpolar Ocean of the Southern Hemisphere (Fig. 5), extending beyond the Antarctic Polar Front. When the temperature of the deepwater is very close to the freezing point of seawater as noted, the upwelling of deepwater does not necessarily result in the significant melting of sea ice. On the other hand, the heat conduction from the bottom of the sea ice to the cold surface is very large, contributing to the growth of sea ice. It is expected that sea ice becomes thick enough until the melting and freezing balance each other.

One is tempted to speculate that sea ice was also very extensive at the LGM as noted by Cook and Hays (1982) and was responsible for the low CO<sub>2</sub> concentration in the atmosphere. As noted by Stephens and Keeling (2000), such extensive and thick sea ice could severely limit the sea-to-air CO<sub>2</sub> flux in the primary region of deepwater ventilation, inducing the low CO<sub>2</sub> concentration in the atmosphere at the last glacial maximum (LGM).

In the 1/2×C experiment, the extensive sea ice described above coexists with a thick layer of Antarctic bottom water with near-freezing temperature. The upwelling of cold deep water beneath very cold air enhances the production of sea ice as it diverges due to the Ekman drift driven by intense surface westerly. The relatively saline surface water, which is produced through increased brine rejection, diverges, occupying the sinking region of the THC in the immediate vicinity of the Antarctic continent. This is why the sinking of saline water and formation of the bottom water are faster in the 1/2×CO<sub>2</sub> than the control experiment as discussed in Sect. 5.2.

As the CO<sub>2</sub> concentration quadruples from the control to the 4×C case, the average temperature of deepwater at the depth of 3 km increases from 1.1 to 6.6 °C. The magnitude of this increase is comparable to the increase of surface air temperature of 5 °C from 23.3 to 28.3 °C in low latitudes (Fig. 3). The result described here differs from what Manabe and Bryan (1985) obtained from their earlier experiment. They found that, in qualitative agreement with the result from the isotopic analysis of deep-sea cores (Savin 1977), the increase of bottom water temperature is comparable to the increase of sea surface temperature at high southern latitudes, but is larger than its increase at low latitudes. In the 4×C experiment, the warming of the bottom water is constrained by the cold air blown off the massive Antarctic ice sheet, which prevents the substantial increase of sea surface temperature above the freezing point in certain regions in the immediate vicinity of Antarctic continent. As indicated by Fig. 6, which illustrates the geographical

**Fig. 4** Latitude-depth distribution of time-mean temperature (°C) zonally averaged over all model oceans. The time mean is taken over the last 100 years of each experiment. *Upper left: the control; lower left: 2×C; upper right: the 1/2×C; lower right: 4×C*

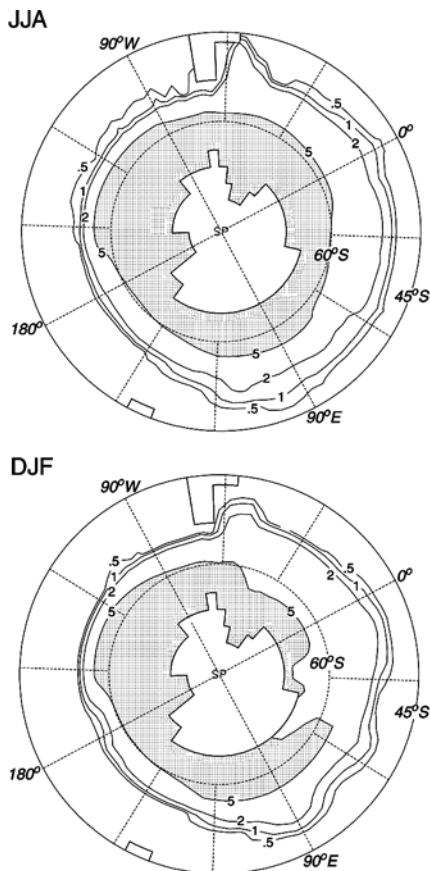
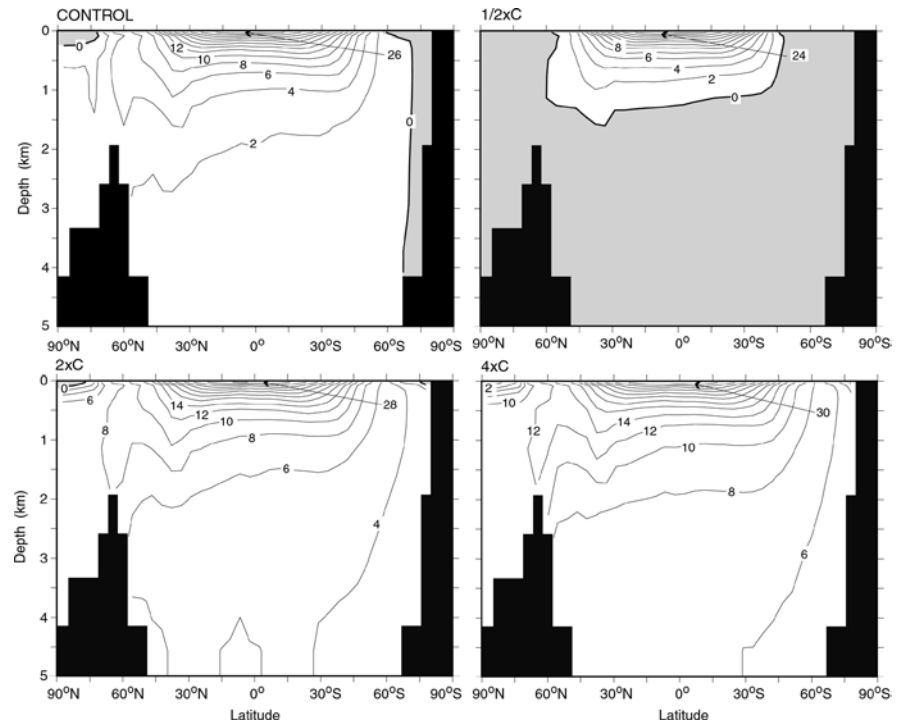


**Fig. 5** The geographical distribution of monthly mean sea ice thickness (m) obtained from the 1/2×C experiment. *Top: June–July–August; bottom: December–January–February*

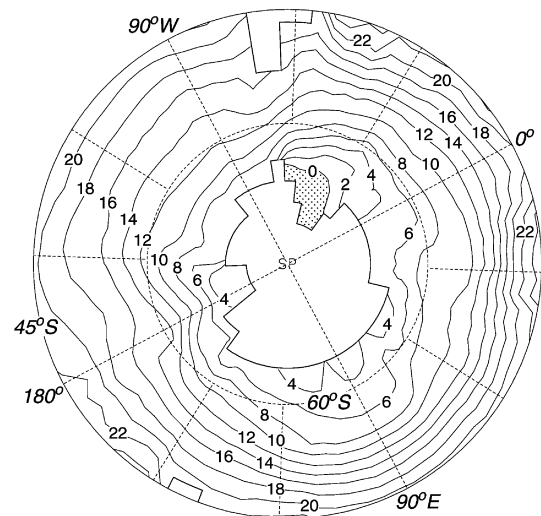


**Fig. 6** Geographical distribution of sea surface temperature (°C) averaged over the last 100 years of the 4×C experiment. *Dashed area in the Weddell Sea indicates the region, where sea surface temperature is below 0 °C. (For economy of space, the distribution of sea surface temperature is illustrated over the region poleward of 45S.)*

distribution of sea surface temperature obtained toward the end of the 4×C experiment, sea surface temperature remains close to the freezing point near the coastal boundary of Weddell Sea, where the formation of Antarctic bottom water predominates. If the Antarctic ice sheet were absent, it is possible that the warming of the Antarctic bottom water would have been larger.

## 5 Thermohaline circulation

### 5.1 Evolution of THC

In the 2×C integration, the THC of the Atlantic Ocean initially weakens. However, as noted in the Introduction, it stopped weakening and regains the original intensity approximately 600 years after the beginning of the experiment, and maintains it during the remainder of the integration, which lasted approximately 4000 years (Fig. 7). In the 4×C integration, the THC in the Atlantic Ocean also weakens initially and becomes very weak after a few hundred years, and remains so until the 1000th year when it starts to intensify (Fig. 7). The sinking Mediterranean water is responsible for maintaining the feeble THC during this period. By the 1750th year, the THC regains the original intensity, and sustains it until the end of the integration, which lasted more than 5000 years. On the other hand, in the 1/2×C integration, the THC intensifies initially but begins to weaken around the 250th year. It keeps weakening, and becomes very weak towards the end of the experiment, which lasts more than 5000 years.

As discussed by Manabe et al. (1991), Manabe and Stouffer (1993, 1994), Wiebe and Weaver (1999), and Dixon et al. (1999), the weakening of the THC during the first few hundred years of the 2×C and 4×C integrations is attributable mainly to the reduction of near-surface salinity of the sub-Arctic and northern North Atlantic oceans. Associated with the warming of the troposphere, the moisture content of air increases, thereby enhancing the poleward transport of water vapor in the troposphere. Thus, precipitation increases by a substantial fraction in high latitudes, contributing to the reduction of salinity and density of near-surface

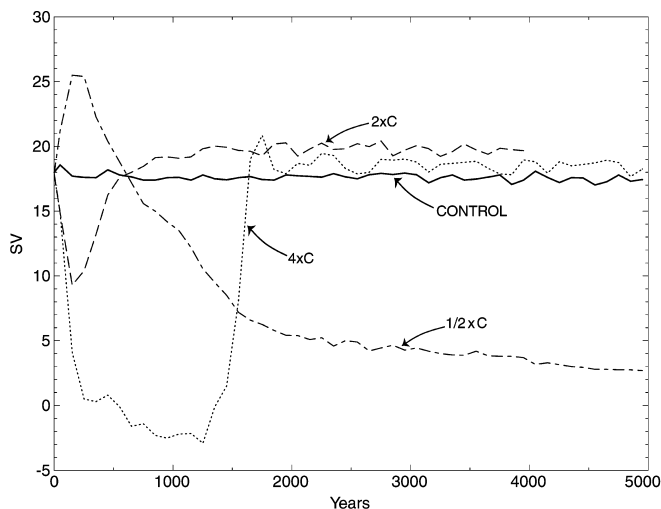


**Fig. 7** The temporal variation of the 100 year-mean intensity of the THC in the Atlantic Ocean. *Solid line*: control; *dashed line*: 2×C; *dotted line*: 4×C; *dash-dotted line*: 1/2×C. Here, the intensity of the THC is defined as the maximum value of its stream function in the North Atlantic Ocean. Units are in Sverdrup ( $= 10^6 \text{ m}^3 \text{ s}^{-1}$ )

water in the Arctic and surrounding oceans. The reduction of the density of near-surface water in turn prevents the convective cooling and sinking of water in northern North Atlantic, thereby weakening the THC. The near-extinction of the THC, which occurred between the 250th and the 1000th years of the 4×C integration, is attributable partly to the development of a thick surface layer of low salinity in the Atlantic Ocean.

In the 1/2×C integration, on the other hand, the temperature and absolute humidity in the troposphere are low, reducing the poleward transport of moisture. Thus, precipitation decreases markedly in high latitudes, thereby reducing the supply of freshwater and ice to Arctic and northern North Atlantic oceans, where surface salinity increases. The increase of surface salinity in turn is responsible for the intensification of the THC in the Atlantic Ocean during the early stage of the 1/2×C integration.

As discussed by Manabe and Stouffer (1993, 1994) and Wiebe and Weaver (1999), the recovery of the THC intensity in the 2×C integration is attributable to the increase in the density contrast between the narrow sinking regions of the THC near Greenland and broad rising regions in low and southern latitudes in the subsurface layer of the North Atlantic Ocean. As explained in Manabe and Stouffer (1993), the increase in the density contrast results mainly from the general increase of temperature in low and southern latitudes. Because of the reduced upwelling of cold water due to the weakening of the THC, a relatively large warming of subsurface layer takes place in these latitudes. Since seawater density depends more upon temperature in low than in high latitudes, the temperature increase in low latitudes results in the increase in density contrast between the rising and sinking regions of the THC.

In the 4×C integrations, the slow recovery of the THC, which began around the 1000th year, is aided by the slow decrease in the static stability of the Atlantic Ocean due to the gradual warming of the bottom water. This gradual warming is due not only to the general increase of sea surface temperature but also to the slowdown in the rate of Antarctic bottom water formation, which results from the reduction of near-surface salinity in the vicinity of the Antarctic continent.

The slowdown of the THC in the 1/2×C integration, which follows its initial intensification, is attributable partly to the reduction in the density contrast between the sinking and rising regions of the THC in the subsurface layer of the Atlantic Ocean. The reduction in the density contrast is attributable partly to the cooling of subsurface water in low and southern latitudes due to the increased upwelling of cold water, which results from the initial intensification of the THC mentioned. At the later stages of the 1/2×C integration, when temperature is reduced markedly in the upper layers of Atlantic Ocean, the density contrast between the cold sinking region and warm rising regions of the THC decreases because the thermal expansion coefficient of seawater decreases with decreasing temperature. The reduction of

the density contrast in turn results in the weakening of the THC, reducing the northward advection of warm, saline water. Towards the end of this integration, a cold upper layer with very low surface salinity develops in the North Atlantic as described in the following subsection, making the THC very feeble.

The results discussed clearly indicate that, in the Atlantic Ocean, the initial trend in the intensity of the THC does not serve as an indicator of the final state to be attained towards the end of an experiment as noted, for example, by Stouffer and Manabe (1999). Although the initial trend is strongly influenced by the change in near-surface salinity, the final state is affected very much by the distributions of not only salinity but also temperature in the deeper layers of the Atlantic Ocean.

## 5.2 Final states of the THC

Figure 8 illustrates the time-mean stream functions of the THC attained towards the end of the various experiments conducted here. It shows that the intensity and distribution of the THC differ little among the control, 2×C, and 4×C cases. On the other hand, the THC in the 1/2×C case is much weaker than other cases. The result described is in qualitative agreement with what Manabe and Bryan (1985) obtained using a coupled ocean–atmosphere model with limited computational domain and idealized geography.

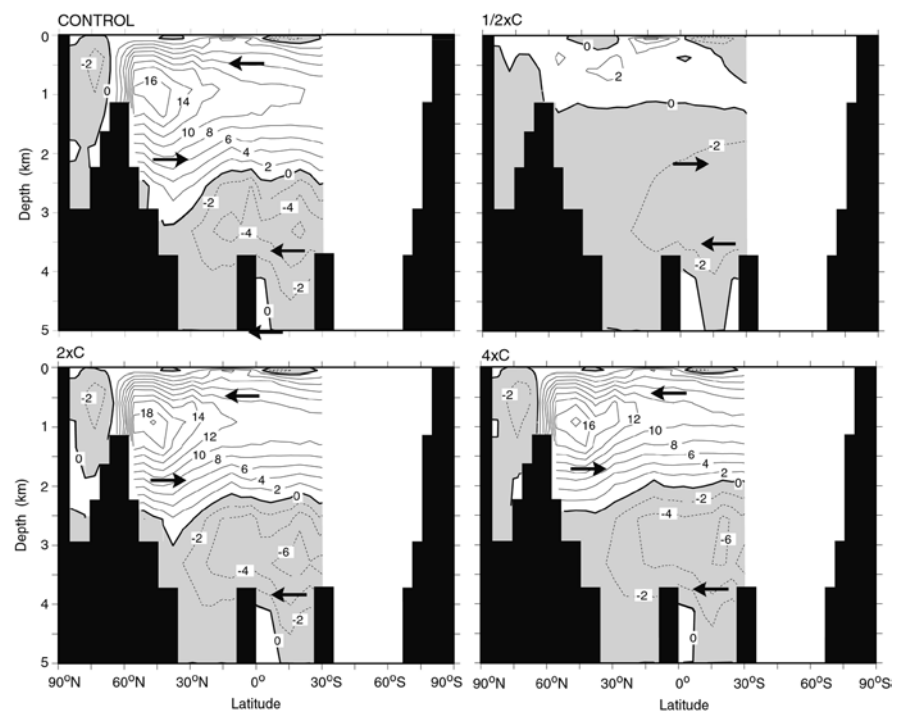
Inspecting Fig. 8, one wonders why the intensity of the THC hardly changes as the CO<sub>2</sub> concentration increases from the standard to four times the standard levels. One could also ask why the intensity decreases so

much from the control to 1/2×C cases. To explore these issues, we constructed Figs. 9, 10 and 11, which illustrate, for the Atlantic Ocean, the distributions of the zonal mean difference in density, temperature, and salinity between the control and other cases.

Figures 9a and 10a indicate that, in the 4×C (or 2×C) case, the density contrast between the sinking and the rising regions of the THC in the subsurface layer (depth range; 0.2–1.0 km) of North Atlantic Ocean is larger than the control case. The larger density contrast is attributable partly to the warmer temperature in the upper layer of ocean, where the thermal expansion coefficient of seawater depends mainly upon temperature. It is attributable also to the increase in temperature contrast in the subsurface layers between the two regions. Because the deepwater is much warmer in the 4×C (or 2×C) than the control case, the vertical gradient of potential temperature is smaller in the former than in the latter case. Thus, the cooling due to the upwelling of deepwater from middle to low latitudes is smaller for the 4×C (or 2×C) than the control case. This is why the subsurface layer is warmer in the 4×C (or 2×C) case from middle to low latitudes of the Atlantic Ocean. The increase of temperature contrast results in the increase in the density contrast between the two regions, enhancing the THC.

Analyzing the results from their 4×C and 2×C experiments, Wiebe and Weaver (1999) attributed the positive temperature anomaly in low latitudes to the small negative buoyancy flux at oceanic surface. In our model results, however, the positive anomaly remains in the subsurface layer, and does not extend to the oceanic surface as Figs. 9b and 10b indicate. We therefore believe that the anomaly is attributable to the reduction

**Fig. 8** The stream function of the THC in the Atlantic Ocean averaged over the last 100 years of each experiment. *Upper left:* the control; *lower left:* 2×C; *upper right:* the 1/2×C; *lower right:* 4×C. Units are in Sverdrup ( $=10^6 \text{ m}^3 \text{ s}^{-1}$ )



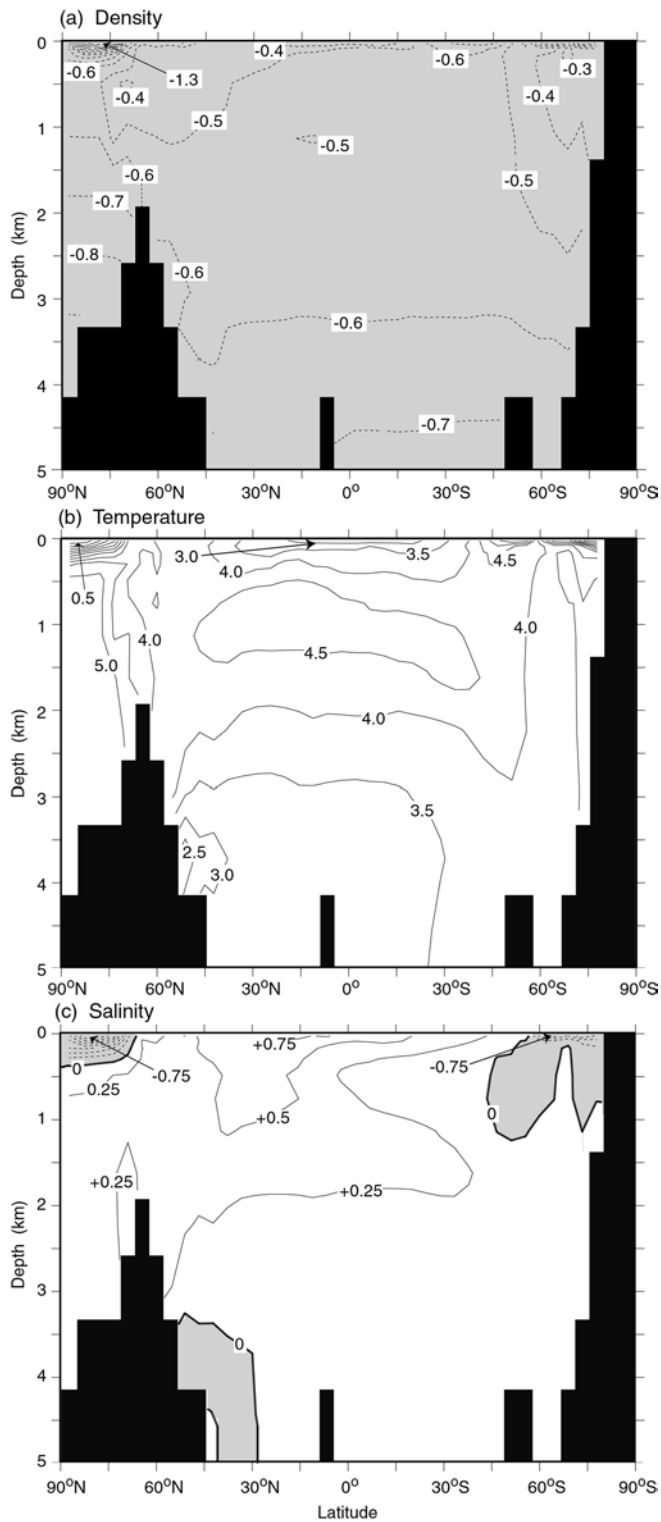


**Fig. 9a–c** Time mean differences in density, temperature and salinity between the 2×C and control experiments, which is zonally averaged over the Atlantic Ocean. **a** Density in parts per thousand; **b** temperature in °C; **c** salinity in psu. Time averaging was made over the last 100 years of each experiment

of the cooling due to the upwelling of deepwater, which is warmer in the 4×C (or 2×C) than in the control experiment.

Opposing the increase in density contrast, which strengthens the THC, there is a factor that tends to weaken the THC. In the warm troposphere of the 2×C and 4×C cases, the absolute humidity of air is high, enhancing the poleward transport of water vapor. Thus, the supply of freshwater to the Arctic and northern North Atlantic increases, contributing to the reduction of near-surface salinity. The thin surface layer of low salinity (and low density) thus produced caps oceanic surface in both 2×C and 4×C cases (Figs. 9c, 10c), weakening the THC. This effect of lower surface salinity in high latitudes counteracts with the effect of the larger density contrast between the sinking and rising regions of the THC described in the preceding paragraph. The net consequence is that the THC is similar among the 4×C, 2×C, and control cases (Fig. 8).

In the 1/2×C case, in which the THC is very weak, the temperature in the upper layer of ocean is much lower than the control case. However, SST in the sinking region of the THC cannot fall below  $-2^{\circ}\text{C}$  due to freezing. On the other hand, SST is reduced markedly from the control to the 1/2×C cases in the broad rising region of the THC. Thus the SST contrast between the two regions is less in the 1/2×C than the control case, weakening the THC.

The marked reduction in the intensity of the THC from the control to the 1/2×C cases, in turn, enhances the contrasts of both temperature and salinity between its sinking region in high northern latitudes and broad rising region in low and southern latitudes in the upper layer of the North Atlantic Ocean (Fig. 11b, c), exerting the opposite influence upon the density contrast. Because the thermal expansion coefficient of seawater decreases with decreasing temperature and becomes very small near the freezing point, a general reduction of temperature contributes to the reduction of the density contrast between the cold sinking and warm rising regions of the THC. This is why the influence of temperature change exceeds that of salinity change, yielding much smaller density contrast in the 1/2×C than the control cases. Thus, the THC is very weak in this case.

Figure 11c indicates that, in middle to high latitudes, salinity in the near-surface layers of the North Atlantic Ocean is much less in the 1/2×C than the control cases. The development of relatively fresh surface layer in the 1/2×C experiment is attributable mainly to the markedly reduced, northward advection of saline surface water from low latitudes. The capping of the sinking regions of the THC by the surface layer with low density weakens the THC further in the 1/2×C case.

It is notable that the THC is not only weak but also shallow in the 1/2×C compared to the control cases. This is because the thick layers of cold bottom water (with temperatures close to  $-2^{\circ}\text{C}$ ) develop, and prevent the deeper penetration of the THC in the Atlantic Ocean. The development of the thick bottom water may be

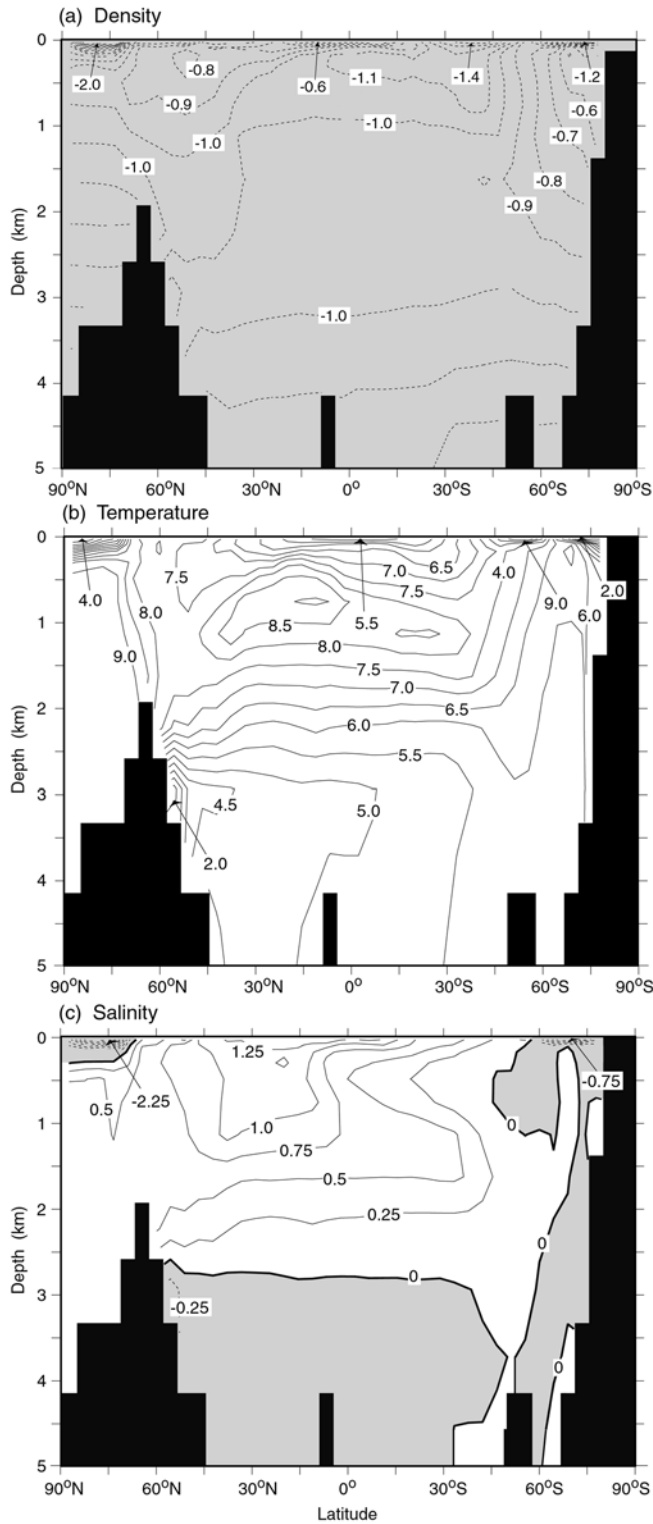


**Fig. 10a-c** Same as Fig. 9, but for the difference between the 4×C and control experiments

attributable to the enhanced production of cold and saline Antarctic bottom water in the Circumpolar Ocean of the Southern Hemisphere. Averaged over the entire latitude circle, the reverse circulation of the bottom

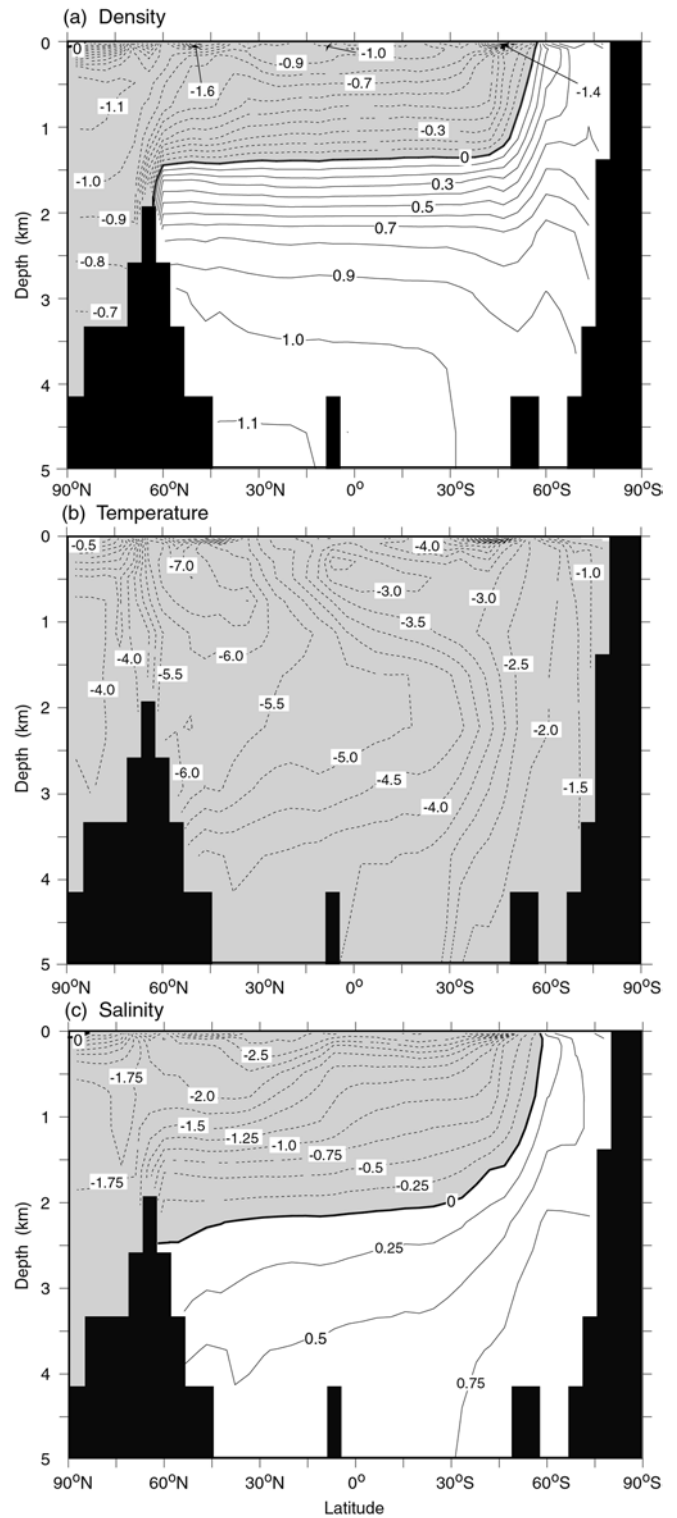


**Fig. 11a-c** Same as Fig. 9, but for the difference between the 1/2×C and control experiments

water is stronger and extends over much a thicker layer in the 1/2×C than control experiments (Fig. 12). The THC in the immediate vicinity of the Antarctic continent is also stronger (Fig. 12), and contributes to the

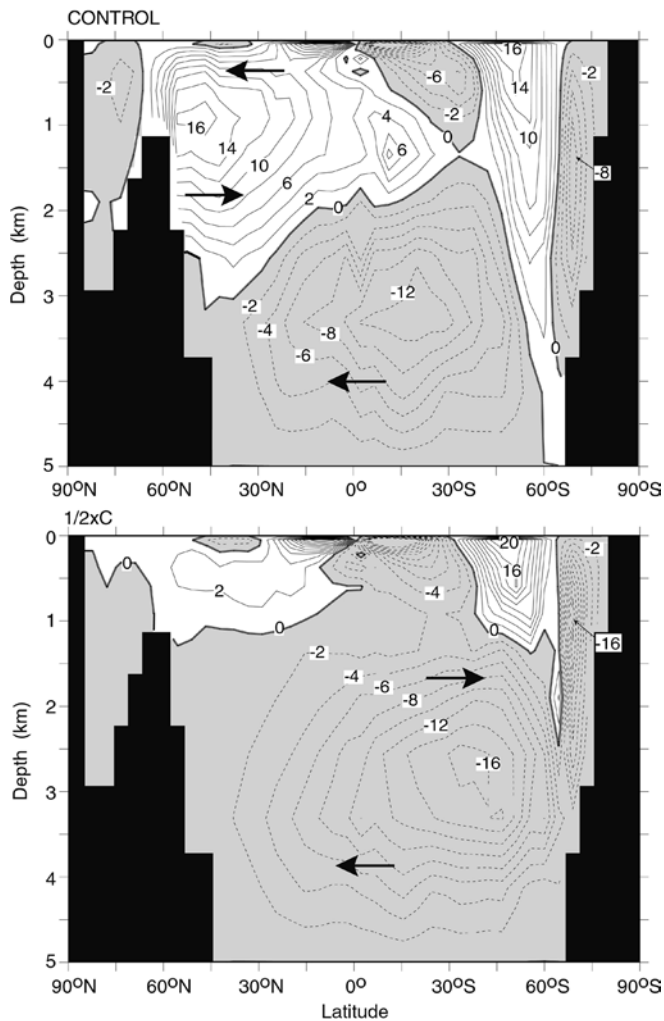


**Fig. 12** The time mean stream function of the meridionally overturning-circulation zonally averaged over all oceans. *Top*: the control experiment; *bottom* the 1/2×C experiment. The time mean is taken over the last 100 years of each experiment

formation of thick layers of bottom water, which prevents the deeper penetration of the THC.

## 6 Inactive mode of THC

Based upon the results from a coupled model, which is very similar to the model used here but has no seasonal variation, Manabe and Stouffer (1988) suggested that, given the standard atmospheric concentration of CO<sub>2</sub>, there are at least two stable modes of the THC in the Atlantic Ocean. In addition to the stable mode of active THC discussed in this study, they found another stable mode of a very weak, reverse THC. This state exhibits very slow rising motion and no ventilation of the entire subsurface water in the North Atlantic Ocean.

However, Schiller et al. (1997) questioned the stability of the reverse THC. Using a coupled model developed at the Max-Planck Institute for Meteorology (MPI),

they produced the reverse THC through the massive discharge of freshwater at the surface of the northwest Atlantic Ocean. Upon termination of the freshwater discharge, however, the THC in the North Atlantic regained its original intensity after a few hundred years. Based upon the results from this numerical experiment, they inferred that the state of the reverse THC with no North Atlantic deepwater formation is not a stable state.

Recently, Manabe and Stouffer (1999) confirmed the existence of two stable modes in their model, using the standard version of their coupled model with seasonal variation of insolation. However, in another version of their coupled model, which uses an unrealistically large coefficient of vertical sub-grid scale diffusion, they found that the mode of reverse THC is not a stable state. (Although the oceanic component of the MPI coupled model has no explicit vertical diffusion, it has large computational diapycnal diffusion, which destabilizes the mode of reverse circulation. For further discussion of this topic, see Manabe and Stouffer 1999.) Here, we show that the stable mode of the reverse THC exists not only for the standard but also four times the standard concentration of CO<sub>2</sub>, when we used the standard version of our coupled model.

To obtain the inactive mode of the reverse THC in the coupled model used here, Manabe and Stouffer (1999) discharged freshwater at the extremely large rate of one Sverdrup (i.e.,  $10^6 \text{ m}^3 \text{ s}^{-1}$ ) over the zonal belt (50°N–70°N) of the North Atlantic Ocean during the initial 100-year period of the control integration of the coupled model. Employing this technique, they were able to reach a stable mode of very weak, reverse THC. Despite the abrupt cessation of the freshwater discharge at the 100th year of the numerical experiment, the THC remains inactive during the remainder of the 12 000-year integration. This result implies that the inactive mode of the THC obtained from the control integration is very close to a stable equilibrium state.

Discharging massive amount of freshwater in an identical manner toward the end of the 4×C integration, when the model ocean approaches very close to the state of equilibrium, we also obtained a stable mode of very weak, inactive THC. Again, the THC remained inactive during the remainder of the 5000-year integration and showed no sign of re-intensification. Although we did not do so, it is likely that we would have obtained a similar, inactive mode of the THC, had we discharged freshwater in a similar manner towards the end of the 2×C experiment.

The stable mode of the reverse THC obtained here differs from the state of very weak THC, which was encountered during the course of the 4×C experiment. In this experiment, the THC became very weak by the 250th year (Fig. 7). However, it started to intensify around the 1000th year, and regains the original intensity by the 1700th year. During the weak phase of the THC, very weak ventilation of deepwater remained due to the sinking of saline water from the Mediterranean Sea. This result indicates that the state of very weak THC obtained in the

4×C integration differs from the stable, inactive mode of reverse circulation, which is obtained here through the massive, discharge of freshwater.

Figure 13 illustrates the inactive modes of THC, which were obtained through the discharge of freshwater for the case of the standard and four times the standard concentrations of atmospheric carbon dioxide. These modes have the weak reverse THC cell with extremely slow upwelling in the North Atlantic and sinking in the southern ocean (not shown). In both cases, the ventilation of deep water is extremely small or non-existent in the entire subsurface layer of the North Atlantic Ocean.

These results indicate that, for the standard and four times the standard concentrations of atmospheric CO<sub>2</sub>, the coupled model has the second stable mode of the inactive THC, if it were forced initially by massive discharge of freshwater over a sufficiently long period of time. Although we discussed mostly the stable mode of

the active THC in this study, it is important to keep in mind that there are at least two stable modes of the THC for not only the standard but also higher CO<sub>2</sub> concentrations in the atmosphere.

No attempt has been made to determine whether the stable reverse THC mode exists for one half the standard CO<sub>2</sub> concentration climate. Nevertheless, we believe it likely that the reverse mode exists for this cold climate. If it does exist, then it may not be very different from the mode of very feeble THC obtained from the 1/2×C experiment. As a matter of fact, the THC was reducing very slowly towards the end of the 1/2×C experiment. Thus it could evidently get into the reverse mode, had we extended the time integration. For CO<sub>2</sub> concentrations lower than half the standard value, we believe it likely that there is only one stable mode: the reverse THC mode.

## 7 Paleocceanographic implications

### 7.1 Deep water formation during Late Tertiary

From the isotopic and faunal analysis of deep-sea cores, Woodruff and Savin (1989) found no evidence for North Atlantic deepwater formation prior to about 14.5 Ma (with the exception of a brief episode in the early Miocene). They found that, from about 10 Ma, the THC was active and resembled the modern circulation with active deepwater formation.

Blanc and Duplessy (1982) proposed that the North Atlantic deepwater formation began around 10–20 Ma as a consequence of the submergence of the Scotland-Faeroe-Iceland-Greenland ridge. On the other hand, Woodruff and Savin (1989) speculated that the onset and acceleration of North Atlantic deepwater formation around the middle Miocene had been related to the increased outflow of saline water from the Mediterranean Sea to the Atlantic Ocean, which resulted from the closure of the connection between the Tethys/Mediterranean basin and Indian Ocean.

In the preceding section, we have shown that, for various CO<sub>2</sub> concentrations of the atmosphere, the coupled model has at least two stable modes of the THC. One mode is a realistic and active THC with narrow, sinking regions near Greenland. The other mode is a reverse THC, which has extremely weak upwelling with no ventilation of the water below the surface in the North Atlantic Ocean. One could speculate that, prior to 14.5 Ma, the North Atlantic Ocean was in a state that resembles the inactive mode of the THC and had no ventilation of deepwater. The various topographic changes, which occurred during the middle Miocene, may be responsible for the transition to active modes of the THC toward the end of the Miocene.

### 7.2 The Younger Dryas event

The isotopic analysis of Greenland ice core (e.g., Grootes et al. 1993) indicates that surface temperature

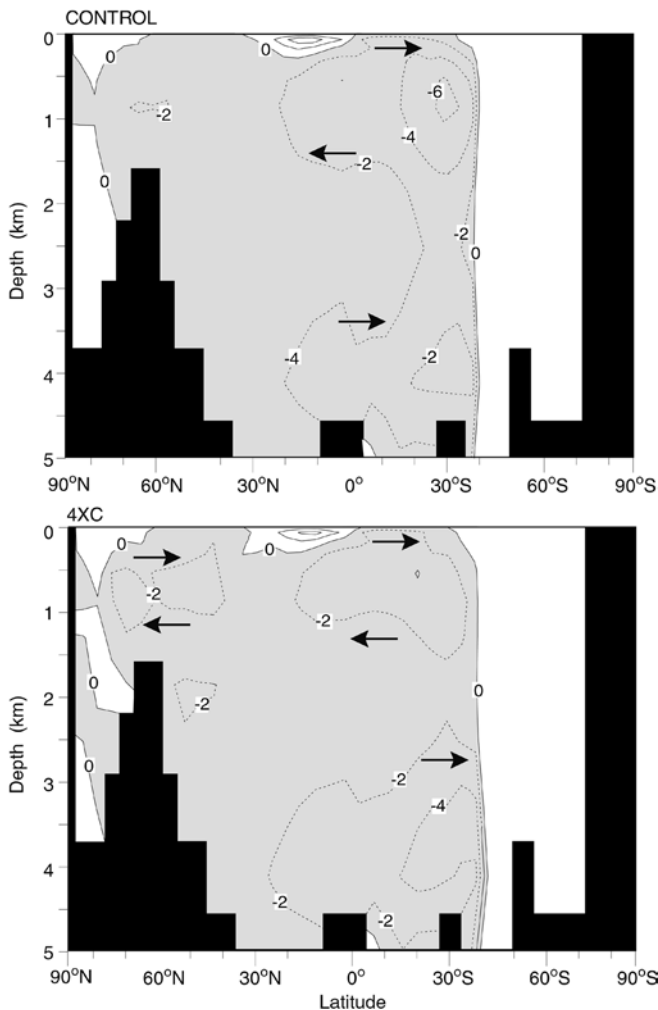


**Fig. 13** The stream functions of the inactive mode of the Atlantic THC induced by the massive, initial discharge of freshwater in the control experiment (*top*) and 4×C experiments (*bottom*). Stream function represents an overturning circulation, which is zonally averaged over the Atlantic Ocean, and is time-averaged over the last 100 years of each experiment. Units are in Sverdrup (i.e.  $10^6 \text{ m}^3 \text{ s}^{-1}$ )

over Greenland dropped very rapidly approximately 13,000 years ago, followed by the Younger Dryas period, when the isotopic temperature was almost as low as the last glacial maximum. The cold period of the Younger Dryas lasted almost 1000 years and ended abruptly (e.g., Alley et al. 1993). Broecker et al. (1985) suggested that such an abrupt change resulted from a very rapid change in the THC from one mode of operation to another. Based upon the result from a set of numerical experiments, Manabe and Stouffer (1988) speculated that the cold period of the Younger Dryas may be a manifestation of the stable, inactive mode of the THC, and the abrupt changes at the beginning and the end of the Younger Dryas period may result from the transition between the two stable modes of the THC in the North Atlantic Ocean.

However, in the experiments described in Sect. 6, the abrupt termination of the massive freshwater discharge was not sufficient to induce the transition from the inactive to the active modes of the THC. As a matter of fact, both the active and inactive modes of the THC are very stable in this model. It takes a very large forcing to make the THC change from one equilibrium state to another so abruptly. Therefore, we no longer believe that the Younger Dryas is a manifestation of the stable, inactive mode of the THC, which is very resistant to change. Instead, we believe that it is indicative of the active mode of the THC, which is temporarily weakened by the massive discharge of continental ice or meltwater. This speculation appears to be consistent with the result of Sarnthein et al. (1994), which indicates that the upper deepwater of the North Atlantic Ocean was ventilated during the Younger Dryas. As suggested by Manabe and Stouffer (2000), the abrupt changes, which occurred at the beginning and end of the Younger Dryas event, may be attributable partly to the multi-decadal oscillation of the THC (Delworth et al. 1993), which is amplified by freshwater discharge with large temporal variability.

### 7.3 The THC at the Last Glacial Maximum

Using a coupled ocean–atmosphere model, in which a highly parameterized model of the atmosphere is coupled with a two-dimensional, zonal mean model of ocean, Ganopolski et al. (1998) made an attempt to simulate the climate of the Last Glacial Maximum (LGM). Forcing their model by a reduced atmospheric CO<sub>2</sub> concentration and imposing the continental ice sheets of the LGM reconstructed by Peltier (1994), they conducted a time-integration of their model over the period of 5000 years, successfully reaching the state of quasi-equilibrium. The THC in the Atlantic Ocean thus obtained was shallower in the LGM than the modern simulation. However, the intensity of the THC from the LGM simulation is slightly weaker than but is comparable to the modern simulations. They note that the similarity in the intensity of the THC between the LGM

and modern simulations is consistent with the radiochemical analysis of deep-sea sediments from LGM, which was conducted by Yu et al. (1996).

Combining a simple energy balance model of the atmosphere with a three-dimensional model of the oceans, Weaver et al. (1998) constructed a coupled model and attempted to simulate the LGM climate. They found that, in the Atlantic Ocean, the THC is shallower in the LGM than modern simulations in agreement with the results of Ganopolski and his collaborators. However, the intensity of the THC is significantly less in the LGM than modern simulations.

Recently, Hewitt et al. (2001) made an ambitious attempt to simulate the state of LGM, using a coupled ocean–atmosphere GCM, which was developed at the Hadley Center for Climate Prediction and Research, United Kingdom. The oceanic component of their model has 2–4 times as high a resolution as that of the coupled model used here and has realistic simulation of the Earth's climate without the use of flux adjustments. Although the coupled model is integrated over the period of 1000 years, the model fails to reach the state of quasi-equilibrium, exhibiting a systematic trend in the distribution of both temperature and salinity toward the end of the time integration. The THC they obtained is shallower than but as intense as the modern simulation.

In the present 1/2×C experiment, the THC is much shallower than the control simulation in qualitative agreement with the results from the modeling studies described. In both the 1/2×C and LGM experiments mentioned, a very thick layer of cold deepwater develops in the bottom half of the Atlantic Ocean, thereby preventing the deeper penetration of the THC. On the other hand, the THC in the 1/2×C experiment is much weaker than the LGM experiments. We shall discuss the reason for the difference.

In the 1/2×C experiment, the halving of the atmospheric concentration of CO<sub>2</sub> results in a climate, which is substantially colder than the LGM climates, which are obtained by other LGM experiments mentioned. At LGM, the CO<sub>2</sub> concentration is about 190 ppm by volume (e.g., Neftel et al. 1982), which is about 1.4 (= square-root of 2 rather than 2) times less than its pre-industrial value of 265 ppm. Reducing the atmospheric concentration of CO<sub>2</sub> by a factor of about 1.4 and including the effect of the continental ice sheets with higher surface albedo, Broccoli and Manabe (1985) found that the global mean surface temperature of their atmosphere-mixed layer ocean model decreased by 4.7 °C. On the other hand, when CO<sub>2</sub> concentration is reduced by a factor of two in the present 1/2×C experiment, the global mean surface temperature is reduced by as much as 7.85 °C (Table 1). As discussed, we believe that very cold SSTs are responsible for the very weak THC obtained from the 1/2×C experiment.

Since SST cannot fall below –2 °C, which is the freezing point of seawater, SST in the sinking region of the THC remains near the freezing point in the 1/2×C experiment. On the other hand, in low and southern

latitudes, where the very broad rising part of the THC is located, the SST is much lower in the 1/2×C than the other LGM experiments. Thus, the temperature contrast between the sinking and rising regions of the THC is much smaller in the 1/2×C experiment. In our opinion, this is why the THC is much weaker in the 1/2×C than other LGM experiments described. In the LGM experiment conducted by Weaver et al. (1998), the THC is significantly weaker than the modern experiment, probably because temperature contrast between the sinking and the rising regions of the THC is smaller.

## 8 Summary and conclusion

Starting from the conditions obtained from the control integration, we have performed here several long integrations (more than 4000 years) using a coupled model. In the 2×C and 4×C integrations, the THC initially weakens, but intensifies later. The final intensity of the THC is similar among the control, 2×C and 4×C experiments. In the 1/2×C integration, on the other hand, the THC initially intensifies, but weakens thereafter, becoming very weak toward the end of the experiment. In short, the initial change of the THC does not necessarily point toward its final equilibrated state. This is because the initial response is dominated by the change in near-surface salinity in the sinking region of the THC, whereas the final response is affected by the changes in not only surface salinity but also the broad scale distribution of temperature and salinity in the Atlantic Ocean. The present study clearly underscores the results from many earlier studies that one should not use the initial transient response as an indicator of the final equilibrium response.

In order to present an overview of the results obtained from this study, we show in Fig. 14 how the intensity of the equilibrated THC depends upon the CO<sub>2</sub> concentration in the atmosphere. This figure indicates that, if the CO<sub>2</sub> concentration is higher than 150 ppm by volume, the coupled model possesses not only an active but also an inactive mode of the THC, which has practically no ventilation of water below the surface in the Atlantic Ocean. On the other hand, if the CO<sub>2</sub> concentration is less than 150 ppm, the coupled model may have only the inactive mode. However, we have not determined whether the coupled model continues to have two stable modes, when the CO<sub>2</sub> concentration becomes much larger than 1200 ppm, which is the highest concentration considered in this study.

One of the important factors, which determine the intensity of the THC, is the temperature dependence of thermal expansion coefficient of seawater. When the temperature of seawater is near its freezing point in high latitudes in the upper layer of oceans, the thermal expansion coefficient of seawater is small, whereas it is large in low latitudes, where the temperature is high. If temperature increases generally in the upper layer of oceans in response to the increase in the atmospheric

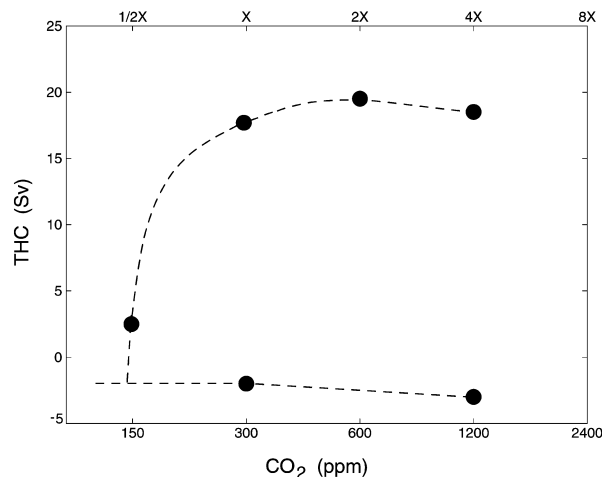


**Fig. 14** The intensities of the THC obtained from the 1/2×C, control (1×C), and 2×C and 4×C are plotted against the CO<sub>2</sub> concentration (in logarithmic scale) in the atmosphere. Units are in Sverdrup ( $=10^6 \text{ m}^3 \text{ s}^{-1}$ ). The dashed line is drawn, smoothly connecting the plots, which represent the final 100-year mean intensities of the THC from all of the experiments conducted here

concentration of CO<sub>2</sub>, the density contrast increases between the cold sinking regions of the THC near Greenland and its warm rising regions in low and southern latitudes, thereby strengthening the THC. This is one of the important reasons why the THC becomes stronger as the CO<sub>2</sub> concentration increases from 1/2×C to 2×C experiments.

On the other hand, there are other factors, which weaken the intensity of the THC as the CO<sub>2</sub> concentration increases in the atmosphere. In a warm troposphere with high CO<sub>2</sub> concentration, the absolute humidity of air is high, maintaining a large poleward transport of water vapor. This yields an ample supply of freshwater to the Arctic and surrounding oceans, and reduces surface salinity, thereby contributing to the weakening the THC in the Atlantic Ocean. This effect becomes relatively more important as the atmospheric concentration of CO<sub>2</sub> increases. This is why the intensity of the THC peaked in the 2×C experiment and becomes slightly smaller in the 4×C experiment.

Inspecting Fig. 14, one notes that the difference in the intensity of the THC is much larger between the 1/2×C and the control than between the control and 2×C cases. This non-linearity in the equilibrium response of the THC to the doubling of the CO<sub>2</sub> concentration appears to be attributable partly to the inability of sea surface temperature to fall below the freezing point of seawater, i.e.,  $-2^\circ \text{C}$ . Thus, the temperature contrast between the sinking and broad rising regions of the THC is limited in the cold 1/2×C case compared with the other cases, and is partly responsible for the nonlinear behavior of the THC response. The large difference in the intensity of the THC between the control and 1/2×C experiments is attributable also to the mutually enhancing relationship between the weakening of the THC and the reduction in the surface salinity in high North Atlantic latitudes.

The intensity of THC obtained from the 1/2×C experiment is much less than the intensities obtained from the three LGM experiments, which were recently conducted, using coupled ocean–atmosphere models of various complexity (Ganopolsky et al. 1998; Weaver et al. 1998; Hewitt et al. 2001). We have found that, in general, SST in the 1/2×C experiment is substantially colder than three LGM simulations mentioned. On the other hand, SST in the sinking region of the THC cannot fall below −2 °C due to the freezing of seawater. Thus, the temperature contrast between the sinking region of the THC in the northern North Atlantic and its broad rising region in the southern oceans is much less in the 1/2×C than the other LGM simulations. It is therefore likely that the smaller temperature contrast described is responsible for the much weaker THC in the 1/2×C as compared to other LGM experiments.

As Fig. 14 indicates, in the control (1×C) and 4×C cases, there are at least two stable modes of the THC in the Atlantic Ocean. One mode has an active THC, which has sinking region in the northern North Atlantic. The other mode has a weak, reverse overturning circulation, which has extremely weak rising motion and practically no ventilation of the entire subsurface water in the North Atlantic Ocean.

Woodruff and Savin (1989) noted that, prior to about 14.5 Ma, North Atlantic deepwater was very poorly ventilated. They noted, however, the rate of the deepwater formation became as large as the modern rate from about 10 Ma. As we speculated in the preceding section, the off and on modes of deepwater formation noted by Woodruff and Savin (1989) may be the manifestation of the two modes of the THC, which we obtained in the present study.

**Acknowledgements** We are very grateful to Tom Delworth, Keith Dixon, and Robby Toggweiler of the Geophysical Fluid Dynamics Laboratory of NOAA and Uwe Mikolajewicz of the Max-Planck Institute of Meteorology, Germany for giving us many useful comments for improving the manuscript. Thanks are due to Jorge Sarmiento of Princeton University, who shared with us his insight on the paleoceanographic implication of the results obtained here. A part of this study was written while Syukuro Manabe was at the Frontier Research System for Global Change, Yokohama, Japan.

## References

- Alley RB, Meese DA, Shuman CA, Gow AJ, Taylor KC, Grootes PM, White JWC, Ram M, Waddington ED, Mayewski PA, Walrus A (1993) Two hold lower snow accumulation rates during the Younger Dryas at the Summit Greenland location. *Nature* 362: 527–529
- Blanc P-L, Duplessy JC (1982) The deepwater circulation during the Neogene and the impact of the Messinian salinity crisis. *Deep Sea Research* 29A: 1391–1414
- Broecker WS, Peteet D, Rind D (1985) Does the ocean–atmosphere system have more than one stable mode of operation? *Nature* 315: 21–25
- Bryan K (1969) Climate and ocean circulation: III. The ocean model. *Mon Weather Rev* 97: 806–827
- Bryan K, Lewis L (1979) A water-mass model of world ocean. *J Geophys Res* 84: 2503–2517
- Cook DW, Hays JD (1982) Estimate of Antarctic Ocean seasonal sea-ice cover during glacial intervals. In: Craddock C (ed) *Antarctic Geoscience: Symposium on Antarctic Geology and Geophysics*, Scientific Committee on Antarctic research, International Union of Geological Sciences, Inter-Union Commission on Geodynamics, August 22–27, 1977, University of Wisconsin Press, Madison, Wisconsin, pp 1017–1025
- Delworth TL, Manabe S, Stouffer RJ (1993) Interdecadal variation of the thermohaline circulation in a coupled ocean–atmosphere model. *J Clim* 6: 1993–2011
- Dixon KW, Delworth TL, Spelman MJ, Stouffer RJ (1999) The influence of transient surface fluxes on North Atlantic overturning in a coupled GCM climate change experiment. *Geophys Res Lett* 26: 2749–2752
- Ganopolsky A, Rahmstorf S, Petroukhov V, Claussen M (1998) Simulation of modern and glacial climates with a coupled global model of intermediate complexity. *Nature* 391: 351–356
- Grootes PM, Stuiver M, White JWC, Johnsen S, Jouzel J (1993) Comparison of oxygen isotope records from the GISP2 and GRIP Greenland ice cores. *Nature* 366: 552–554
- Gordon CT, Stern W (1982) A description of the GFDL global spectral model. *Mon Weather Rev* 110: 625–644
- Hall A, Stouffer RJ (2001) An abrupt climate event in a coupled ocean–atmosphere simulation without external forcing. *Nature* 409(6817): 171–174
- Hewitt CD, Broccoli AJ, Mitchell JFB, Stouffer RJ (2001) A coupled model study of the last glacial maximum: was part of the North Atlantic relatively warm? *Geophys Res Lett* 28(8): 1571–1574
- Intergovernmental Panel on Climate Change (1991) The IPCC scientific assessment. In: Houghton JT, Jenkins GJ, Ephraums JJ (eds) *Climate Change*. Cambridge University Press, Cambridge, UK
- Intergovernmental Panel on Climate Change (1995) *Climate change 1995: the science of climatic change*. In: Houghton JT, Meira Filho LG, Callander BA, Harris N, Kattenberg A, Maskell K (eds) Cambridge University Press, Cambridge, UK
- Intergovernmental Panel on Climate Change (2001) *Climate change 2001: the scientific basis*. In: Houghton JT, Ding Y, Griggs DJ, Mougner M, van der Linden PJ, Dai X, Maskell K, Johnson CA (eds) Cambridge University Press, Cambridge
- Manabe S (1969) Climate and ocean circulation I. The atmospheric circulation and the hydrology of the earth's surface. *Mon Weather Rev* 9: 739–774
- Manabe S, Broccoli AJ (1985) A comparison of climate model sensitivity with data from the last glacial maximum. *J Atmos Sci* 42: 2643–2651
- Manabe S, Bryan Jr K (1985) CO<sub>2</sub>-induced change in a coupled ocean–atmosphere model and its paleoclimatic implications. *J Geophys Res* 90: 11,689–11,707
- Manabe S, Stouffer RJ (1988) Two stable equilibria of thermohaline circulation. *J Clim* 1: 841–866
- Manabe S, Stouffer RJ (1993) Century-scale effects of increased atmospheric CO<sub>2</sub> on the ocean–atmosphere system. *Nature* 364: 215–218
- Manabe S, Stouffer RJ (1994) Multiple century response of a coupled ocean–atmosphere model to an increase of atmospheric carbon dioxide. *J Clim* 7: 5–23
- Manabe S, Stouffer RJ (1999a) The role of thermohaline circulation in climate. *Tellus* 51A–B: 91–109
- Manabe S, Stouffer RJ (1999b) Are two modes of thermohaline circulation stable? *Tellus* 51A: 400–411
- Manabe S, Stouffer RJ (2000) Study of abrupt climate change by a coupled ocean–atmosphere model. *Quat Sci Rev* 19: 285–299
- Manabe S, Smagorinsky J, Strickler RF (1965) Simulated climatology of a general circulation model with a hydrologic cycle. *Mon Weather Rev* 93: 769–798
- Manabe S, Stouffer RJ, Spelman MJ, Bryan K (1991) Transient response of a coupled ocean–atmosphere model to a gradual change of atmospheric CO<sub>2</sub> Part I: annual mean response. *J Clim* 4: 785–818

- Marotzke J, Stone P (1995) Atmospheric transport, the thermohaline circulation and flux adjustments in a simple climate model. *J Phys Oceanog* 25: 1350–1364
- Neftel AH, Oeschger H, Schwander J, Stauffer B, Zumbunn R (1982) Ice core sample measurements give atmospheric CO<sub>2</sub> content during the past 40 000 yr. *Nature* 295: 220–223
- Peltier WR (1994) Ice age paleotopography. *Science* 265: 195–201
- Sarnthein M, Winn K, Jung SA, Duplessy J-C, Labeyrie L, Erlenkeuser H, Gaussen G (1994) Changes in east Atlantic deepwater circulation over the past 30,000 years: eight times slice reconstruction. *Paleoceanography* 9: 209–267
- Savin SM (1977) The history of earth's surface temperature during the past 100 million years. *Annual Rev Earth Planet Sci* 5: 319–355
- Schiller A, Mikolajewicz U, Voss, R (1997) The stability of the North Atlantic thermohaline circulation in a coupled ocean-atmosphere general circulation model. *Clim Dyn* 13: 325–347
- Schrag D, Hampt PG, Murray DW (1996) Pore Fluid constraints on the temperature and oxygen isotopic composition of the glacial ocean. *Science* 272: 1930–1932
- Spelman MJ, Manabe S (1984) Influence of oceanic heat transport upon the sensitivity of a model climate. *J Geophys Res* 89(C1): 571–586
- Stephens BB, Keeling RF (2000) The influence of Antarctic sea ice on glacial-interglacial CO<sub>2</sub> variations. *Nature* 404: 171–174
- Stouffer RJ, Manabe S (1999) Response of a coupled ocean-atmosphere model to increasing atmospheric carbon dioxide: sensitivity to the rate of increase. *J Clim* 12: 2224–2237
- Stouffer RJ, Manabe S, Bryan K (1989) Interhemispheric asymmetry in climate response to a gradual increase in CO<sub>2</sub>. *Nature* 342: 660–662
- Weaver AJ, Eby M, Fanning AF, Wiebe EC (1998) Simulated influence of carbon dioxide, orbital forcing and ice sheets on the climate of the last glacial maximum. *Nature* 394: 847–853
- Wiebe EC, Weaver AJ (1999) On the sensitivity of global warming experiments to the parameterization of sub-grid scale mixing. *Clim Dyn* 15: 875–893
- Woodruff F, Savin SM (1989) Miocene deepwater oceanography. *Paleoceanography* 4: 87–140
- Yu E-F, Francois R, Bacon MP (1996) Similar rates of modern and last glacial ocean thermohaline circulation inferred from radiochemical data. *Nature* 379: 689–694